Comparison of Linear and Nonlinear H-Infinity Controllers for an Electric Vehicle Driven by the Permanent Magnet Synchronous Motor

F. Oudjama[1], A. Boumédiène[2], M. Messirdi[3] and D. Boubekeur[4]
[1]Ph.D. Student, GEE Department,
LAT, Laboratoire d'Automatique de Tlemcen, Université de Tlemcen 13000, Tlemcen, Algeria.
[2]Professor, GEE Department,
LAT, Laboratoire d'Automatique de Tlemcen, Université de Tlemcen 13000, Tlemcen, Algeria.
[3]Ph.D. Student, GEE Department,
LAT, Laboratoire d'Automatique de Tlemcen, Université de Tlemcen 13000, Tlemcen, Algeria.
[4]Lecturer, Oran 1 University, Oran, Algeria,
MELT, Manufacturing Engineering Laboratory of Tlemcen, Tlemcen, Algeria.

(Corresponding author: F. Oudjama)

ABSTRACT: The electric vehicle driven by the permanent magnet synchronous motor system has been considered as the best choice for numerous applications. To make electric vehicle a high performances drive, effective control system is required. The linear and nonlinear H∞ controller's strategies are designed to improve robustness, tracking performances of the electric vehicle and disturbance rejection. For linear systems, the H∞ controller is obtained by solving the algebraic Riccati equation. However, the nonlinear H-infinity controller control problem requires the solution of the Hamilton-Jacobi-Isaacs (HJI) equation which is a nonlinear partial differential equation that is generally difficult or impossible to solve, and may not have global analytic solutions even in simple cases. The successive Galerkin Approximation (SGA) technique provides an approximation to the solution of the Hamilton-Jacobi equations associated with the nonlinear H-Infinity control theory that produces stabilizing, closed-loop control law with well-defined stability regions. The simulations of Electric Vehicle responses for both nonlinear and linear H∞ controllers will be performed and compared assure efficiency comportment in all type of constraints. It is found that the nonlinear H∞ controller has a similar performances and robustness than the linear controller. Despite all of the electric vehicle nonlinearities the linearized approach work adequately, however, the full nonlinear approach proves to be better for this application.

Keywords: Electric Vehicle, Hamilton-Jacobi-Isaacs equation, H-infinity robust control, Nonlinear, Successive Galerkin Approximation.

Abbreviations: EV, electric vehicle; HJI, hamilton-jacobi-isaacs equation; H∞, H-infinity robust control; SGA, successive galerkin approximation.

I. INTRODUCTION

By definition, an electric vehicle is a vehicle whose propulsion is provided by an engine operating exclusively with electrical energy [1, 2, 3]. The electric vehicle is advanced by all players in the automotive field, because it's classified as one of the cleanest and most environmentally friendly transport solutions. Indeed, it could be an alternative to this alarming pollution, especially since the road transport sector emits more pollutants into the atmosphere than the industry sector. However, despite the extensive research on the power train and batteries, the electric vehicle is still expensive and is subject to modification or improvement [4].

With the progress of automatic, computer, telecommunications and miniaturization of instruments, researchers are now able to develop driving assistance systems that automate certain tasks in order to improve safety by increasing the stability of the electric vehicle, in which, the systems must act on the controllability of

the electric vehicle so that the latter responds more quickly to the demands of the driver.

Furthermore, the dynamics of the Electric Vehicle driven by the PMSM is inherently nonlinear due to inertial coupling, aerodynamic effects, and the actuator complex model. The controller designs is typically based on linearized dynamics models, the nonlinearities of the Electric Vehicle significantly affect the dynamic response. Many control methods have been proposed for Electric Vehicle autopilot design in the past. such as classical control laws [1, 2, 5, 6, 7], and for more advanced algorithms using for example fuzzy logic control [5, 8, 9,10], nonlinear control [11,12], sliding mode control [5,13, 14], back stepping control [15,16], and H∞ control [17,18,19, 20, 21, 22, 23]. Unfortunately, as yet, even though modern control theories, and post-modern control methodologies, have become very sophisticated, there is no best solution for this problem. Among the methods that have been investigated are nonlinear robust control design approaches based on

the solutions to the Hamilton-Jacobi-Isaacs (HJI) equations, respectively. However solving these two partial differential equations analytically is very difficult and the quest for a reliable and accurate approximation of its solution is an open problem. The Successive Galerkin Approximation (SGA) method is used to approximate the solution of the Hamilton-Jacobi-Isaacs (HJI) equations, using a stabilizing feedback controller was computed offline [24, 25].

In this paper, A Galerkin approximation to the nonlinear H∞ problem is studied and compared with the results of a linearized H∞ control for electric vehicle driven by the PMSM. These control strategies are chosen for their performance. It is well known that the solution of the linear *H∞* control problem depends upon by solving algebraic Riccati equation [26, 27, 28]. For the nonlinear *H∞* controller requires the solution of the Hamilton-Jacobi-Bellman (HJB) equation [29-34]. This partial differential equation is very difficult to solve, and the quest for a reliable and accurate approximation of its solution is an open problem. The Successive Galerkin Approximation (SGA) is one such method of approximation to accomplish the approximation of the Hamilton-Jacobi-Bellman equations are first reduced to an infinite sequence of linear partial differential equations, named generalized Hamilton-Jacobi-Bellman equations. Second, Galerkin's method is used to approximate the solutions of these linear equations, and the combination of these two steps yields a control algorithm that converges to the optimal solution as the order of the approximation and the number of iterations goes to infinity [29, 30, 31].

After introduction section, the organization of this work is as follows. In section II, the electric vehicle studied is presented and modeled, so we give it a state space representation. Section III describes the design of the linear and nonlinear H∞ control, and the Galerkin successive approximation method. In section IV we analyze our design approach and its application to the electric vehicle. In Section V, the designed controller is implemented and numerically simulated, and the performances are evaluated. Section 6 provides the conclusions of this study.

II. PROBLEM DESCRIPTION

In this study, the Electric Vehicle model driven by the permanent magnets synchronous motor is considered. The single-motor configuration with a mechanical transmission composed by a differential more gearing or without gearing as shown in Fig. 1 [1].

A. Modeling of vehicle dynamics
The vehicle dynamic model can be determined by the summation of all the forces applied on it, given by Newton's second law [1, 2, 6]. According to Fig. 2, the total resistance force consists of rolling resistance, aerodynamic resistance, and gravitational force. Hence, the resultant force is the sum of all acting forces, and is given by Fig. 2.
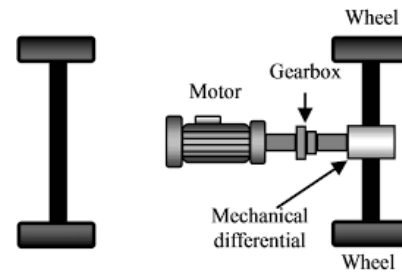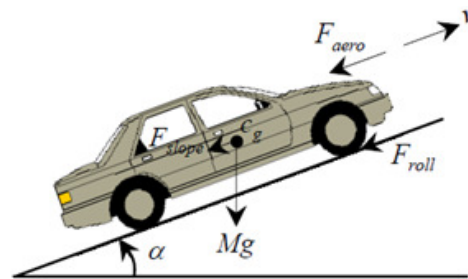

Fig. 1. The configuration of the EV.

Fig. 2. Forces applied on a vehicle.

The total resultant force is the sum of all acting forces, and it is given by: $F = F_g + F_{aero} + F_{roll} + M\dfrac{dV}{dt}$ (1)

• The gravitational force can be expressed as:

$$F_g = Mgsin(\alpha)$$ (2)

• The aerodynamic resistance force is a function of vehicle speed *V*, and it is expressed as:

$$F_{aero} = \frac{1}{2}\rho A_f C_D V^2$$ (3)

• The rolling resistance force is primarily due to the friction of the vehicle tires on the road and can be expressed as:

$$F_{roll} = M\ g\ f_r \cos(\alpha)$$ (4)

The resultant force *F* will produce a counteractive torque to the driving motor, which is governed by the following relationship:

$$T_L = F \times \frac{r}{G}$$ (5)

The relation between the linear speed V of the EV and the angular speed Ω_{mot} of the motor is shown by:

$$V = \frac{r}{G}\Omega_{mot}$$ (6)

Where r is the wheel radius, Ω_{mot} is the motor rotation speed and T_L the torque produced by the driving motor.

B. PMSM Model
The permanent magnet synchronous motor is defined in the rotor *dq* reference frame can be described by the following equations [38, 39]:

$$\frac{di_d}{dt} = -\frac{R}{L}i_d + P\Omega_{mot}i_q + \frac{1}{L}u_d$$

$$\frac{di_q}{dt} = -\frac{R}{L}i_q - P\Omega_{mot}i_d + \frac{P\Phi}{L}\Omega_{mot} + \frac{1}{L}u_q \quad (7)$$

$$\frac{d\Omega_{mot}}{dt} = \frac{3P\Phi}{2J}i_q - \frac{B}{J}\Omega_{mot} + \frac{T_L}{J}$$

In Equation (7), u_d, u_q and i_d, i_q are stator voltages and currents in the *dq* reference frame respectively; R is the stator resistance, L is inductance in the *dq* reference frame, P is the pole pairs, Φ is the permanent magnet flux, J moment of inertia of the motor, B is the viscous friction coefficient and T_L is the load torque [38, 39, 40].

So combing the model of PMSM and the vehicle dynamic model, the overall dynamic model of the EV system can be written as:

$$\dot{x}_1 = -\frac{R}{L}x_1 + \frac{PG}{r}x_2x_3 + \frac{1}{L}u_d$$

$$\dot{x}_2 = -\frac{R}{L}x_2 - \frac{PG}{r}x_1x_3 - \frac{P\Phi G}{Lr}x_3 + \frac{1}{L}u_q$$

$$\dot{x}_3 = \frac{1}{J_v}\begin{bmatrix} \frac{3P\phi G}{2}x_2 - \frac{BG}{r}x_3 - \frac{r}{G} \\ \left(Mgsin(\alpha) + Mgf_r\cos(\alpha) + \frac{r^2}{2G^2}\rho A_f C_D x_3^2\right) \end{bmatrix}$$

$$(8)$$

With : $J_v = \dfrac{JG^2 + mr^2}{rG}$

Where x is the state vector which takes the forms of

$x = [x_1, x_2, x_3]^T = [i_d, i_q, v]^T$; u is the control input which is given by u_d and u_q

To develop the nonlinear *H∞* controller for the EV, first, the nonlinear model of the EV in (8) needs to be transformed to the appropriate error dynamics.

The speed error, the *d–q* axis current errors, and the desired *q*-axis current can be defined as [41, 42]:

$$e_1 = x_1 - x_{1d} \quad e_2 = x_2 - x_{2d} \quad e_3 = x_3 - x_{3d} \quad (9)$$

$$x_{2d} = \frac{2J_v}{3P\phi G}\dot{x}_{3d} + \frac{r^3\rho A_f C_D}{3J_v P\phi G^4}x_{3d}^2 + \frac{2BG}{3P\phi Gr}x_{3d}$$

$$+ \frac{r}{3J_v P\phi G^2}\left(Mgsin(\alpha) + Mgf_r\cos(\alpha)\right) \quad (10)$$

Where x_{2d} is the desired speed, e_3 is the vehicle speed error, e_2 and e_1, are the *q*-axis and *d*-axis current errors, respectively.

Next, the control signals u_{ds} and u_{qs} can be decomposed into the following compensating and stabilizing terms:

$$u_d = u_{ds} + u_{dc} \ , \ u_q = u_{qs} + u_{qc}$$

Where u_{ds} and u_{dc} are the *d*-axis stabilizing and compensating control terms, and u_{qs} and u_{qc} are the *q*-axis stabilizing and compensating control terms, respectively

The compensating control terms u_{dc} and u_{qc} are defined as:

$$u_{qc} = -\frac{LPG}{r}x_2x_3 \quad (11)$$

$$u_{dc} = -\frac{LPG}{r}x_{2d}x_{3d} \quad (12)$$

Fig. 3 shows a schematic diagram of the proposed linear and nonlinear H∞ controller.

Using (8) to (12), the vehicle dynamic model (8) can be expressed as the following error dynamics

$$\dot{e}_1 = -\frac{R}{L}e_1 + \frac{1}{L}u_{ds}$$

$$\dot{e}_2 = -\frac{R}{L}e_2 - \frac{P\Phi G}{Lr}e_3 + \frac{1}{L}u_{qs} \quad (13)$$

$$\dot{e}_3 = \frac{1}{J_v}\begin{bmatrix} \frac{3P\phi G}{2}e_2 - \frac{\rho A_f C_D r^3}{2G^3}e_3^2 - \\ \left(\frac{BG}{r} + \frac{\rho A_f C_D r^3}{G^3}x_{3d}\right)e_3 \end{bmatrix}$$
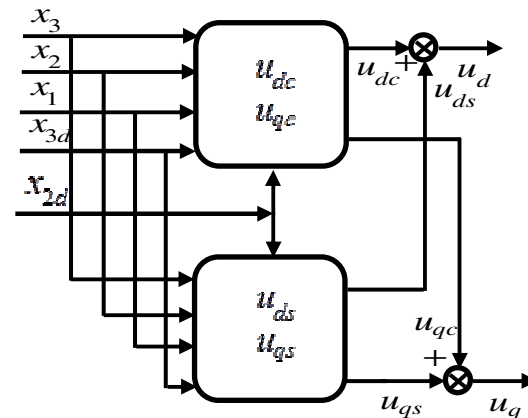

Fig. 3. Schematic diagram of the proposed linear and nonlinear H∞ controller.

III. H∞ CONTROL DESIGN

A. The linear H∞ controller

Let us consider the following affine nonlinear continuous-time dynamical system [29-34]:

$$\dot{x} = f(x) + g(x)u + k(x)w$$

$$z = \begin{bmatrix} h(x) \\ u \end{bmatrix} \quad (14)$$

where $x \in \Re^n$ is the vector of the system's state variables, $w \in \Re^q$ is the vector of exogenous inputs, $u \in \Re^m$ is the vector of control inputs and $z \in \Re^s$ is the vector of exogenous outputs which characterizes the control objective. The mappings $f(x)$, $g(x)$, $k(x)$ and $h(x)$ are assumed to be nonlinear smooth functions and,

for simplicity, $f(0) = h(0) = 0$.

The linearized model of the nonlinear continuous-time dynamical system described in (14) is represented by:

$$\begin{cases} \dot{x}(t) = Ax(t) + B_2 u(t) + B_1 w(t) \\ \qquad\quad y = Cx(t) \end{cases} \qquad (15)$$

Where:

$$A = \left.\frac{\partial f(x)}{\partial x}\right|_{x=0}, \; B_1 = k(0), \; B_2 = g(0), \; C = \left.\frac{\partial h(x)}{\partial x}\right|_{x=0}$$

there exists a controller if and only if a real, symmetric, positive-definite matrix X satisfying the following Ricatti equation exists [26, 27, 28, 29,30].:

$$XA + A^T X + X\left(B_2 B_2^T - \gamma^{-2} B_1 B_1^T\right)X + C_1^T C_1 = 0$$

B. The nonlinear H∞ controller

The nonlinear *H∞* control problem aims to find a controller $u = u(x,t)$ such that the systems (14) is stable and has $L2 - gain \leq \gamma$ from the exogenous inputs ω to the controlled output z [31, 32, 33, 34, 35, 36]:

$$\int_0^\infty \|z\|_2^2 \, dt = \gamma^2 \int_0^\infty \|\omega\|_2^2 \, dt \qquad (16)$$

The system that verifies (16) is also called a dissipative system with the supply rate

$$s(z,\omega) = \frac{1}{2}\gamma^2 \|\omega\|_2^2 - \frac{1}{2}\|z\|_2^2 \qquad (17)$$

Equation (16) is interpreted as a minimization of the ratio between the energy of the controlled output z and the energy of the exogenous input ω.

Consider the nonlinear system of equation (14) and a real parameter $\gamma > 0$ Suppose that exists a smooth positive definite solution, $V(x) > 0$, to the HJI inequality given by equation (18),

$$\begin{aligned} H(x) &= \frac{\partial V}{\partial x}(x)f(x) + \frac{1}{2}h^T(x)h(x) - \frac{1}{2}\frac{\partial V}{\partial x}(x) \\ &\quad \left(g(x)g^T(x) - \frac{1}{\gamma^2}k(x)k^T(x)\right)\frac{\partial^T V}{\partial x}(x) < 0 \end{aligned} \qquad (18)$$

Then, the closed-loop system with the feedback expressed as:

$$u(x) = -\frac{1}{2}g^T(x)\frac{\partial V}{\partial x}(x) \qquad (19)$$

is asymptotically stable at the origin and has locally $L2 - gain$ (from W to Z) less or equal to γ. Moreover, the worst-case disturbance is given by equation (20).

$$w(x) = \frac{1}{\gamma^2}k^T(x)\frac{\partial V}{\partial x}(x) \qquad (20)$$

Generally (18) is very difficult to solve, so an approximate solution is considered. However, the Galerkin's successive approximation (SGA) is one such approximation method.

The successive Galerkin approximation technique for the Hamilton-Jacobi Isaacs (HJI) equation is developed in [35, 36, 37]. The basic idea requires two nested iterations in policy space corresponding to the min - max problem associated with the nonlinear control is given in Algorithm

We begin, with an initial stabilizing control law and then the inner-loop updates the disturbance $\omega(i,j)$ until it is the best strategy for the maximizing player. Then, the outer-loop updates the control, iteratively compute the worst disturbance for the new control, until it is the best strategy for the minimizing player.

Input : N a positive integer,

$\qquad \varepsilon$ a small positive real number

Input : $u^{(0)}(x)$ an initial stabilizing control law,

$\qquad \Omega$ stability region

Input : $A_1, A_2(u^{(0)}(x)), b_1, b_2(u^{(0)}(x))$,

$\qquad \{G_j\}_{j=0}^\infty, \{K_j\}_{j=0}^\infty, i = 0,...N$

Input : $\Phi(x)$ the basis functions

set γ

set c^{old_1}, c^{old_2} ;

for $i = 0$ to ∞ *do*

$\qquad$ set $\omega^{(i,0)} = 0$

$\qquad$ *if* $i == 0$ *then*

$\qquad\qquad A^{(i)} = A_1 + A_2(u^{(0)}(x))$

$\qquad\qquad b^{(i)} = b_1 + b_2(u^{(0)}(x))$

$\qquad$ *else*

$\qquad\qquad A^{(i)} = A_1 - \frac{1}{2}\sum_{k=1}^N c_k^{(i-1,\infty)} G_k$

$\qquad\qquad b^{(i)} = b_1 - \frac{1}{4}\sum_{k=1}^N c_k^{(i-1,\infty)} G_k c_k^{(i-1,\infty)}$

$\qquad$ *end*

$\qquad$ *for* $j = 0$ *to* ∞ *do*

$\qquad\qquad$ *if* $j == 0$ *then*

$\qquad\qquad\qquad A = A^{(i)} \; b = b^{(i)}$

$\qquad$ *else*

$\qquad\qquad\qquad A^{(i)} = A_1 - \frac{1}{2\gamma^2}\sum_{k=1}^N c_k^{(i,j-1)} G_k$

$\qquad\qquad\qquad b^{(i)} = b_1 - \frac{1}{4\gamma^2}\sum_{k=1}^N c_k^{(i,j-1)} G_k c_k^{(i,j-1)}$

$\qquad$ *end*

Solve for $V(i,j)$ from : $c^{(i,j)} = A^{-1}b$

$\qquad$ *if* $\left\|c^{(i,j)} - c^{old_1}\right\| \leq \varepsilon$ *then*

$\qquad\qquad j = \infty$

$\qquad$ *else*

$\qquad\qquad\qquad\qquad\qquad\qquad\qquad\qquad +$

$$c^{old}_1 = c^{(i,j)}$$

$$\textit{end}$$

$$\textit{end}$$

if $\left\| c^{(i,\infty)} - c^{old}_2 \right\| \le \varepsilon \; \textit{then}$

$$i = \infty$$

$$\textit{else}$$

$$c^{old}_2 = c^{(i,\infty)}$$

Update the Disturbance :

$$w(i, j+1) = \frac{1}{2\gamma^2} k^T(x)\nabla\Phi^T c^{(\infty,\infty)}$$

$$\textit{end}$$

Update the Control:

$$u(i+1) = \frac{1}{2} g_2^T(x)\nabla\Phi^T c^{(\infty,\infty)}$$

$$\textit{end}$$

If there is convergence of c,

then reduce γ and go back to step 3

IV. APPLICATION OF THE H∞ CONTROLLER

This section describes the applications of the linear H∞ and nonlinear H∞ controller to the nonlinear electric vehicle driven by the permanent magnet synchronous motor system given in Equation (8). The control objective is to design an asymptotically stable controller for an EV, and to make the EV speed and d-axis current follow the reference signals. Fig. 4 shows the global scheme of the proposed controller.

The design procedure in H∞ control requires a linear model of the system. Therefore, the nonlinear Eq. 9 is linearized using the Taylor's series expansion around its equilibrium point. The linearized error dynamics model of the EV is obtained:

$$\begin{cases} \dot{x}(t) = Ax(t) + B_u u(t) + B_w w(t) \\ y = Cx(t) \end{cases}$$

Where x is the state vector which takes the forms of $x = [x_1, x_2, x_3]^T = [e_1, e_2, e_3]^T$; u is the control input ; w is the disturbance input of the system. The matrices A, B_u, B_w and C of the state space model can be described as follows

$$A = \begin{bmatrix} -\dfrac{R}{L} & 0 & 0 \\ 0 & -\dfrac{R}{L} & -\dfrac{P\Phi G}{Lr} \\ 0 & \dfrac{1}{J_v}\dfrac{3P\phi G}{2}e_2 & -\dfrac{1}{J_v}\left(\dfrac{BG}{r} + \dfrac{\rho A_f C_D r^3}{G^3}x_{3d}\right) \end{bmatrix}$$

$$B_u = \begin{bmatrix} \dfrac{1}{L} \\ \dfrac{1}{L} \\ 0 \end{bmatrix}, B_w = \begin{bmatrix} 1 \\ 1 \\ 0 \end{bmatrix}, C = \begin{bmatrix} 1 & 0 & 1 \end{bmatrix}$$
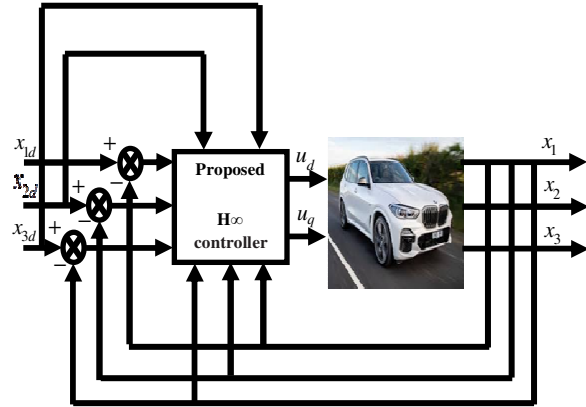
Fig. 4. Block diagram of overall EV driving system.

Solving the corresponding Riccati equation, the following stabilizing state feedback control is obtained:

$$u_{dsL}(x) = -0.9917x_1 - 5.2611 10^{-6}x_2 - 0.9999x_3$$

$$u_{qsL}(x) = -5.2611 10^{-6}x_1 - 4.2997 10^{-9}x_2 - 9.3352 10^{-6}x_3$$

In order to construct a nonlinear H∞ controller, The successive Galerkin approximation technique for the Hamilton-Jacobi Isaacs (HJI) equation was applied to the electric vehicle driven by the permanent magnet synchronous motor system, we used the following initializing parameters: the stability region Ω, the basic functions $\Phi(x)$ and an initial stabilizing H∞ control $u^{(0)}(x)$. In this paper, we used:

$$\Omega = [1.2, 1.2]^3$$

$$\Phi(x) = \left[x_1^2, x_2^2, x_3^2, x_1x_2, x_1x_3, x_2x_3\right]$$

$$u^{(0)}(x) = \left[u_{ds0}(x), u_{qs0}(x)\right] \text{ where}$$

$$u_{ds0}(x) = -0.9917x_1 - 5.2611 10^{-6}x_2 - 0.9999x_3$$

$$u_{qs0}(x) = -5.2611 10^{-6}x_1 - 4.2997 10^{-9}x_2 - 9.3352 10^{-6}x_3$$

After 20 iterations, the algorithm converges to

$$u_{dsNL}(x) = -0.9917x_1 - 3.9741 10^{-20}x_2 - 3.7796 10^{-17}x_3$$

$$u_{qsNL}(x) = -3.9741 10^{-20}x_1 - 3.7593 10^{-5}x_2 - 0.0589x_3$$

This is a nonlinear H∞ control law in feedback strategy form. It is given in terms of the state variables

V. SIMULATIONS RESULTS

Simulations have been carried out to validate the effectiveness and the performances of the nonlinear H∞ robust control compared to the linear H∞ robust control applied to the described model of EV presented in Fig. 4. Several results are obtained under motoring of the EV with nominal parameters given in Table 1 and Table 2.

In Firstly case simulation, the vehicle speed starts from zero to the chosen reference speed 80km/h. A good tracking of the speed can be observed in Fig. 5. The vehicle reaches the reference speed without overshoot. Fig. 6 and Fig. 7 illustrated the behavior of the equivalent stator currents Id and Iq respectively. The stator quadrature current Iq reached 14, 24 A, at to the steady-state. Whereas, it can be seen that d-axis current Id is decoupled from motor torque and regulated to tend toward zero at the settling time of the speed response. The electromagnetic torque generated during the simulation response is shown in Fig. 8, knowing that it is directly proportional to the stator quadrature current Iq.

(b)

Fig. 6.   Id-axis current for Case 1.

(a)

(b)
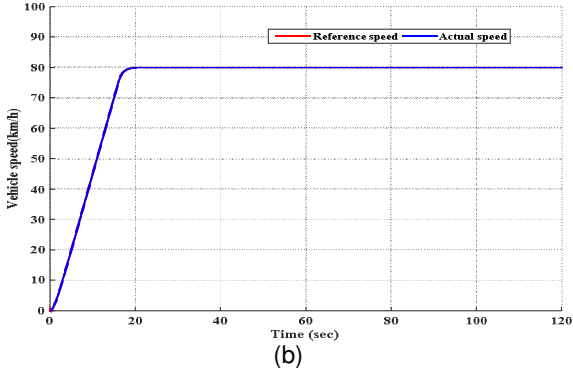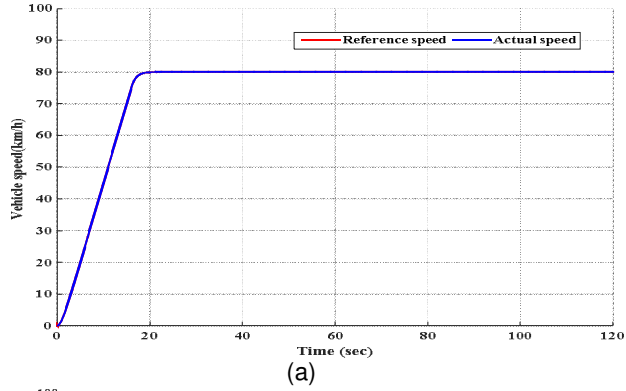
Fig. 5. Vehicle linear speed for Case 1.

(a)

(a)

(a)
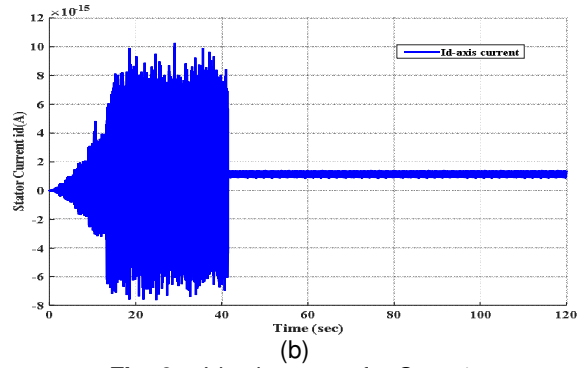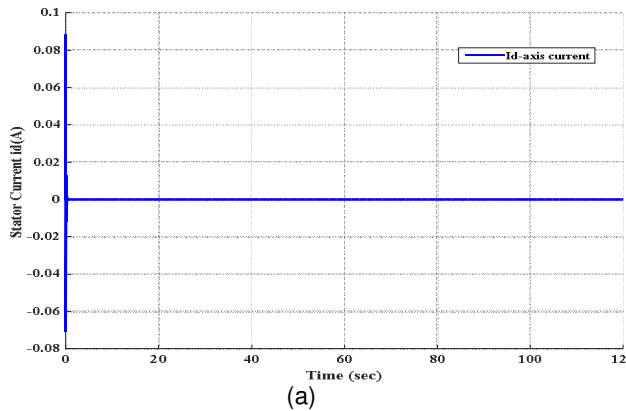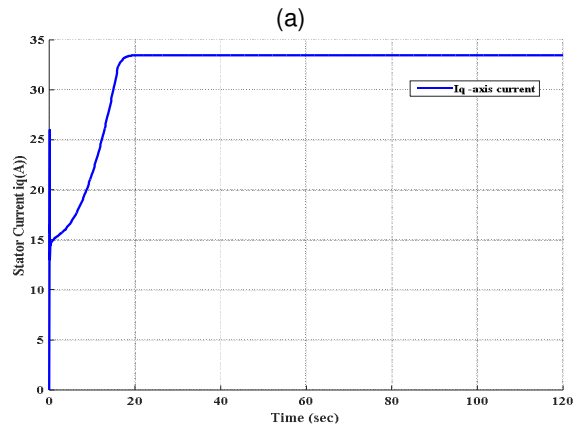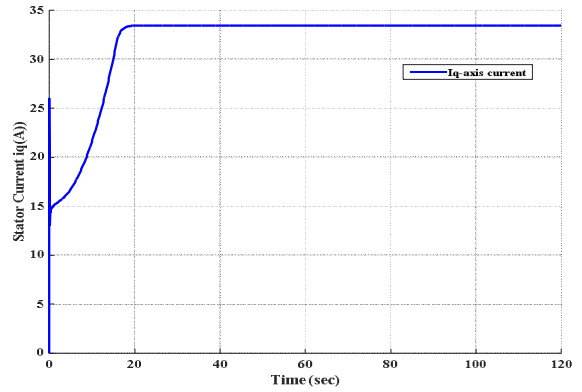
Fig. 7.   Iq -axis current for Case 1.

(a)

(b)
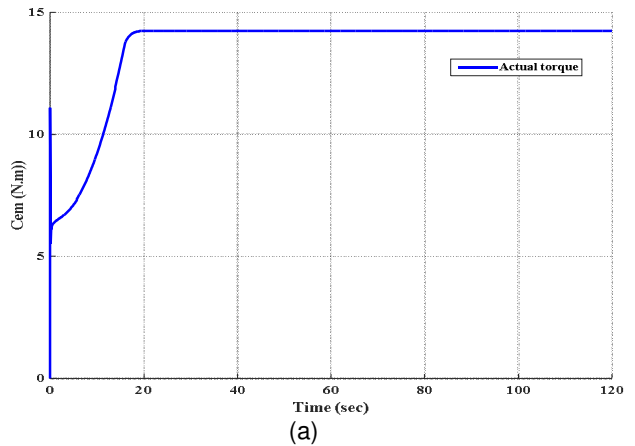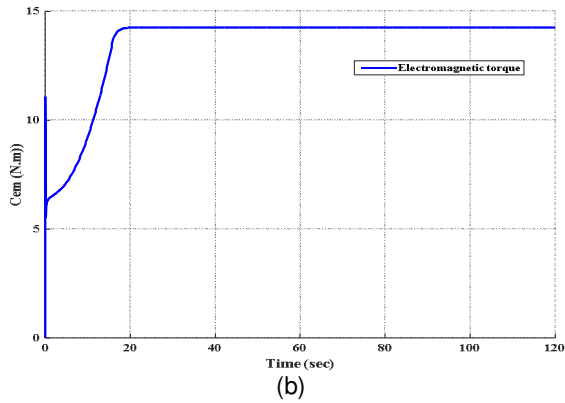
Fig. 8. Electromagnetic torque for Case 1.

(b)

Fig. 9. Vehicle linear speed for the benchmark Case 2.

In the second simulation case, when the vehicle is moving in straight line in a smooth way applying acceleration and deceleration to the vehicle through the accelerator pedal. During this variation, it's clear that the speed shows excellent tracking at the reference speed with an insignificant error rate. For $0 \leq t \leq 60s$ the speed of electric vehicle increases from 0 km/h to 80 km/h, we notice a good tracking of the speed. see Fig. 9. The Fig. 10 show a high electromagnetic torque during the startup of the EV until the final value and settle around 14.25 Nm, Fig. 12 and Fig. 13 illustrates the variations of phase currents and voltages, in which we notice high phase currents and voltages for moving the vehicle from startup until the steady state. At this time, the variations of phase currents and phase voltages begin to increase and then stabilize at 157.14V and 27.32 A. For $60 \leq t \leq 120s$ the speed of the electric vehicle is decreases from 80 km/h to 40km/h the electromagnetic torque decrease also to 23.56 Nm. The phase voltages and currents decrease to the new values 78.11V and 15.82 A. The shape and the magnitude of the electromagnetic torque the phase currents of the motors and the phase voltages of the motors depend on the reference speed.
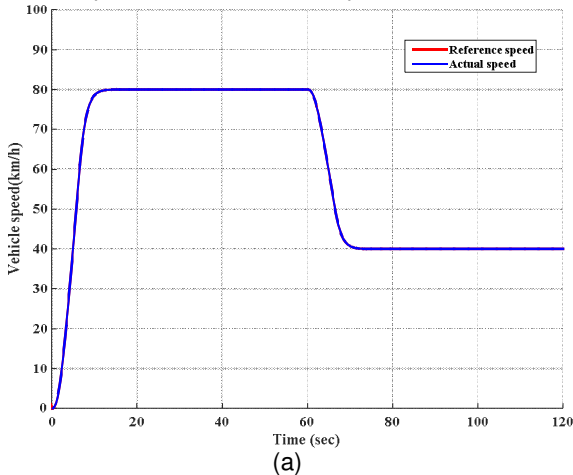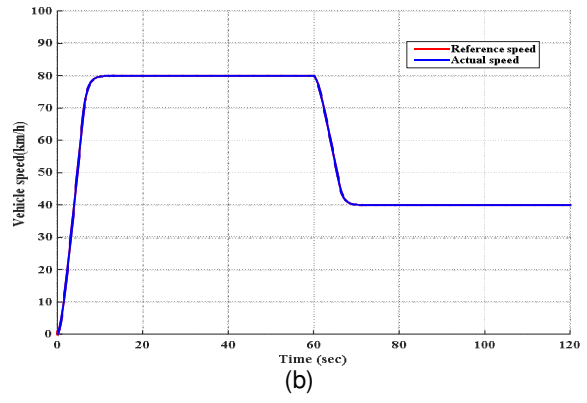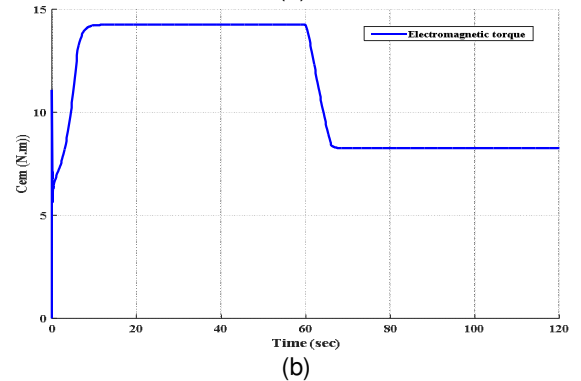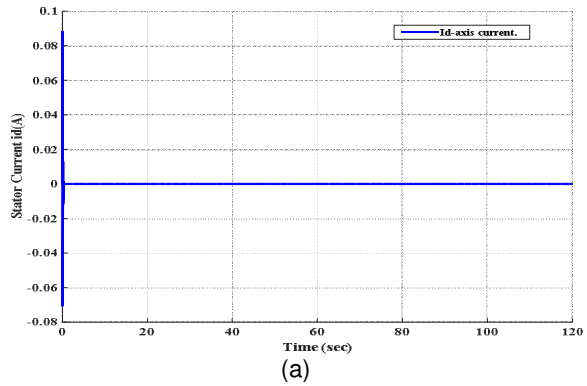

(a)

(b)
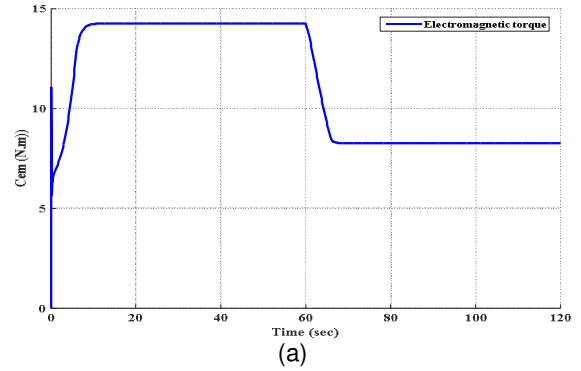
Fig. 10. Electromagnetic torque for the benchmark Case 2.
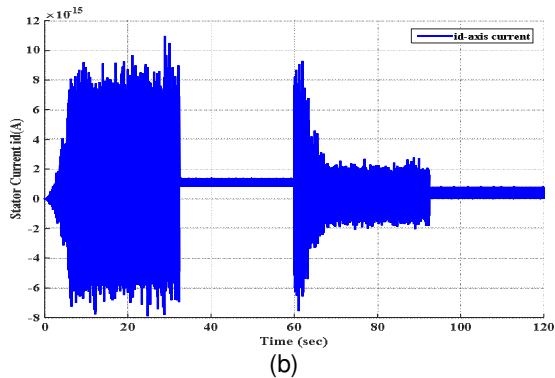

(a)

(a)

(b)

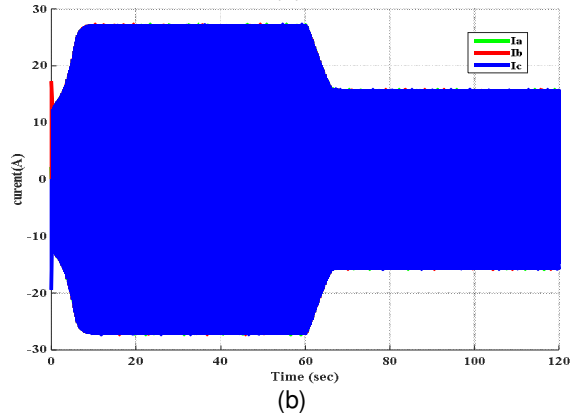**Fig. 11.** id-axis currentfor the benchmark Case 2.

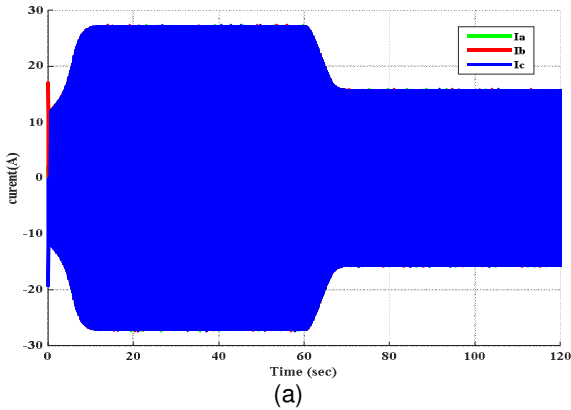

(a)

(b)

Fig. 12. Phase currents of the motors for the benchmark Case 2.
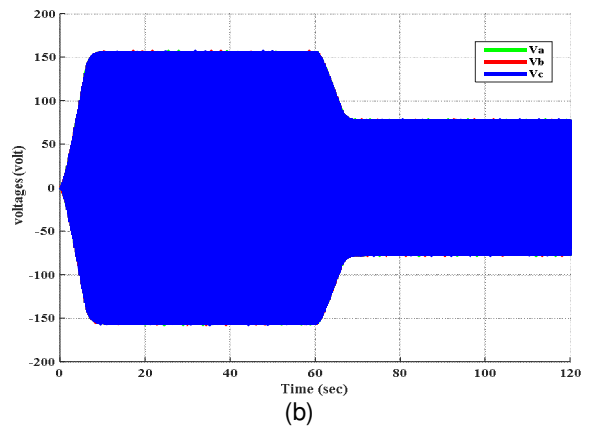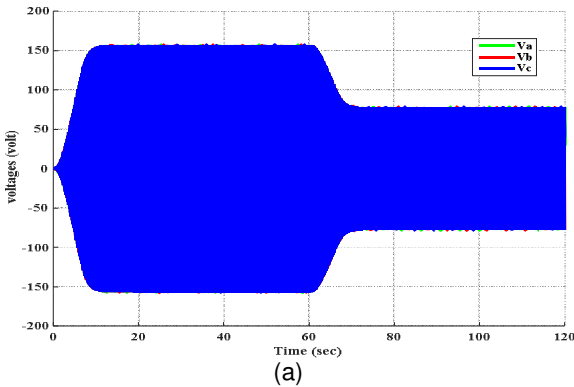

(a)

(b)

Fig. 13. Phase voltages of the motors for the benchmark Case 2.

In Thirdly case simulation is performed with the presence of a slope at t=40 s until t=100s. this test shows the influence of the road slope on the vehicle speed, moving on straight road with 10% slope. The road slope does not affect the speed control of the electric vehicle. According to Fig. 14, only a change of the electromagnetic torque (Fig.15), phase currents (Fig. 17) and phase voltages (Fig. 18) are noticed. The motor develops more and more electromagnetic torque to reach 106.59 Nm, the phase voltages and the phase currents increase speedily to the maximal value 204.3A and 223.5V respectively.
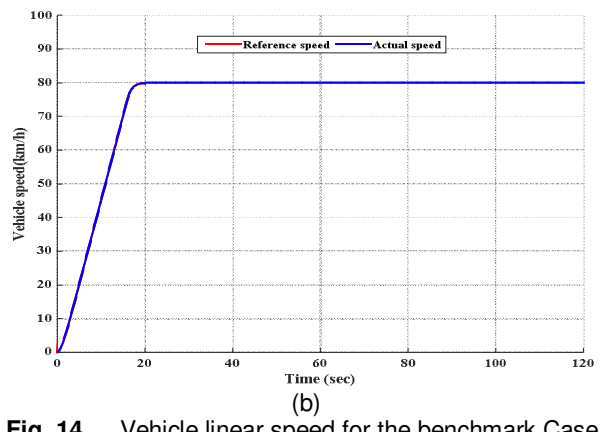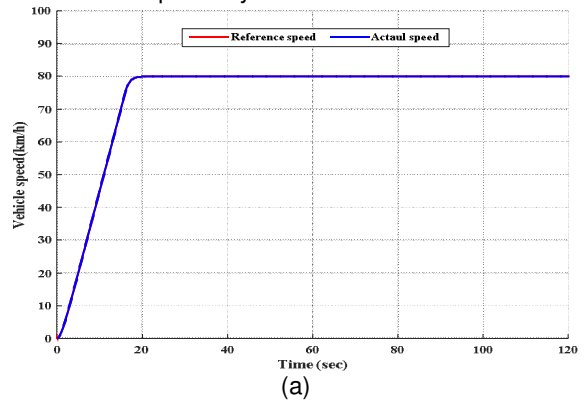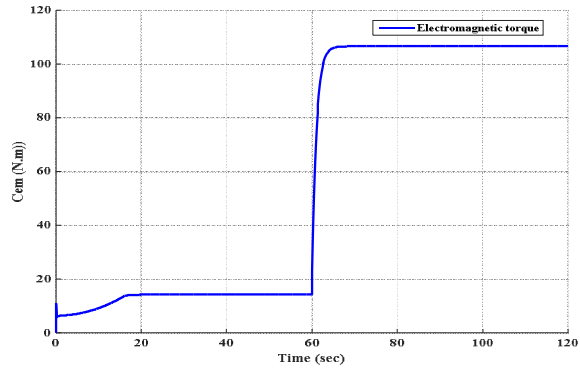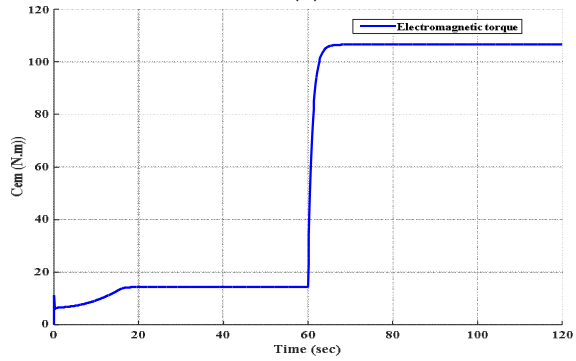

(a)

(b)

Fig. 14. Vehicle linear speed for the benchmark Case 3.

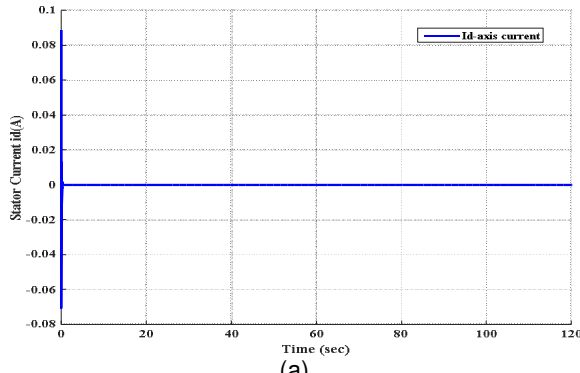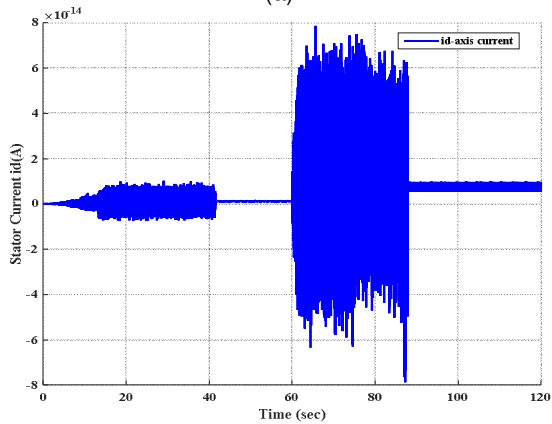**Fig. 15.** Electromagnetic torque for the benchmark Case 3.

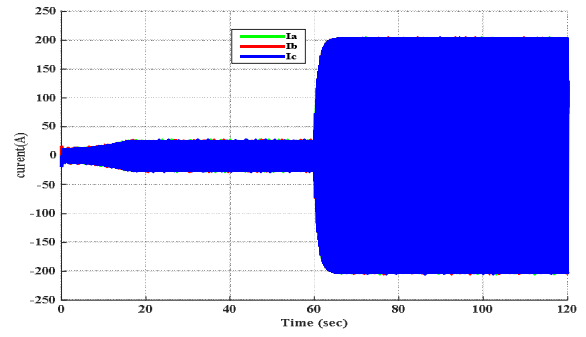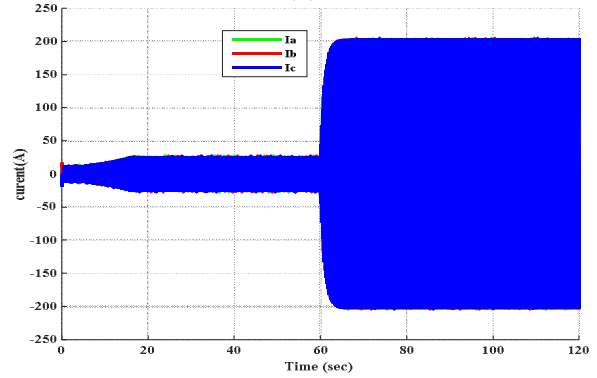**Fig. 16.** id-axis current for simulation Case 3.

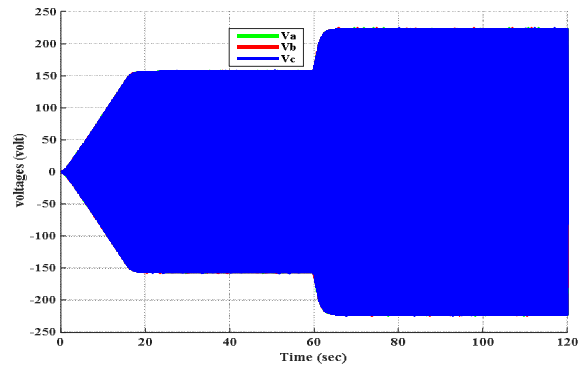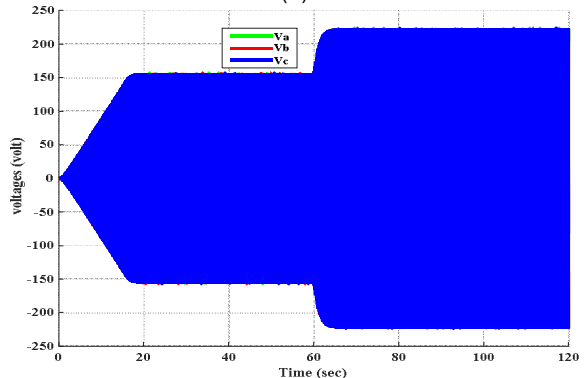**Fig. 17.** Phase currents of the motors for simulation Case 3.

Fig. 18. Phase voltages of the motors for simulation Case 3.

The objectives of the stabilization and tracking for electric vehicle driven by the permanent magnet synchronous motor system have been reached, the system is first controlled to track a speed reference. Next the disturbance rejection ability of the control system is tested by applying acceleration and deceleration of de speed reference and by the presence of a slope. It can be observed that the EV returns to the regulated state very quickly. In general, the speed tracking control is not affected and shows a similar performance using both nonlinear and linear H∞ controllers. As the figures show, the two methods demonstrate nearly the same dynamic behavior with the robust technique for the nonlinear and linear H∞ control applied on nonlinear dynamical system.

The successive Galerkin approximations to the HJI equations produce control algorithms that efficiently regulate the nonlinear Electric Vehicle driven by the PMSM. The performance of this algorithm is superior to the performance of a linearized H∞ controller[19,20,21]. as well as a Fuzzy control, vector control and the Sliding mode control [7].

VI. CONCLUSION

In this paper, a linear and nonlinear H∞ robust control has been developed for speed tracking of electric vehicle driven by the Permanent Magnet Synchronous Motor with the objective to guarantees the robustness propriety, disturbance rejection and ensure better performance while trying to improve the dynamics of the EV. For the linearized equivalent model of the electric vehicle a linear H-infinity feedback controller was designed. The computation of the controller's feedback gain required the solution of an algebraic Riccati equation. Moreover, in order to construct a nonlinear H∞ control approach, the Successive Galerkin Approximation (SGA) technique provides an approximation to the solution of the Hamilton-Jacobi equations is used to design the nonlinear H-infinity controller, then, we apply the algorithm on the electric vehicle driven by the permanent magnet synchronous motor system. The simulations results show a similar performance using both nonlinear and linear H∞ controllers. A good tracking of the vehicle speed and the components Id is regulated using the field control, so, Id is zero. ensure their capacity to maintain ideal trajectories for speed control and ensure good disturbances rejections with no overshoot, eliminates all the unwanted disturbances in the system, and it decreases the settling time, therefore, makes the system faster and more accurate and stabile. It can be concluded that the nonlinear and linear H∞ robust control are a valid method for the control of electric vehicle and give good performances.

VII. FUTURE SCOPE

Future research could be done to determine Nearly optimal control laws for Electric Vehicle Driven by the Permanent Magnet Synchronous Motor using a neural network HJB approach.

REFERENCES

[1]. Schaltz, E., Seref, S. (2011). Electrical Vehicle Design and Modeling. *Electric Vehicles - Modelling and Simulations Journal*, 1 ed., pp. 1-24.
[2]. Mi, C., Abul Masrur, M. (2017). Hybrid Electric Vehicles: Principles and Applications with Practical Perspectives, 2nd Edition.
[3]. D.D., Vafaeipour, M., El Baghdadi, M., Barrero, R., Van Mierlo, J., & Hegazy, O. (2019). Thorough state-of-the-art analysis of electric and hybrid vehicle power trains: Topologies and integrated energy management strategies. Renewable and Sustainable Energy Reviews, 109596.
[4]. Daina, N., Sivakumar, A., & Polak, J.W. (2017). Electric vehicle charging choices: Modelling and implications for smart charging services. *Transportation Research Part C: Emerging Technologies*, *81*, 36–56.
[5]. Aktas, M., Awaili, K., Ehsani, M., & Arisoy, A. (2020). Direct torque control versus indirect field-oriented control of induction motors for electric vehicle applications. *Engineering Science and Technology, an International Journal*.
[6]. Salem, A. (2013). Modeling and control solutions for electric vehicles. *European Scientific Journal*, vol. *9*, No.15.
[7]. Zhang, X., Zhang, Q. and Shi, L. (2012). Development Review of Drive Motor Applied in Electric Vehicle. *Advanced Materials Research*, vols. 433-440, pp 7333-7337.
[8]. Makrygiorgou, J.J., Alexandridis, A.T. (2017). Fuzzy logic control of electric vehicles: Design and analysis concepts. *Twelfth International Conference on Ecological Vehicles and Renewable Energies.*
[9]. Al-Jazaeri, A.O., Samaranayake, L., Longo, S., and Auger, D.J. (2014). Fuzzy Logic Control for energy saving in Autonomous Electric Vehicles. *IEEE International Electric Vehicle Conference*.
[10]. Cheng, S., Yu, J., Zhao, L., & Ma, Y. (2020). Adaptive fuzzy control for permanent magnet synchronous motors considering input saturation in electric vehicle stochastic drive systems. Journal of the Franklin Institute.
[11]. El Majdoub, K., Giri, F., Ouadi, H., and Chaoui, F. Z. (2013). Nonlinear Cascade Strategy for Longitudinal Control of Electric Vehicle. *Journal of Dynamic Systems, Measurement, and Control*, doi: 10.1115/1.4024782.
[12]. Huang, Q., Huang, Z., Zhou, H. (2009). Nonlinear optimal and robust speed control for a light-weighted all-electric vehicle.*IET Control Theory & Applications*, *3*(4), 437–444.
[13]. Lin, C., Peng, C.L. (2013). Stability Control for Dual-Motor Independent Drive Electric Vehicle Based on Sliding Mode Control. *Advanced Materials Research*, 655-657, 1403–1409.
[14]. Gair, S., Cruden, A., McDonald, J., Hredzak, B. (2004). Electronic differential with sliding mode controller for a direct wheel drive electric vehicle. *Proceedings of the IEEE International Conference on Mechatronics*.

[15]. Depature, C., Lhomme, W., Sicard, P., Bouscayrol, A., Boulon, L. (2017). Backstepping Control of an Electric Vehicle with Local Control Saturation. *IEEE Vehicle Power and Propulsion Conference*.

[16]. Nasri, A., Gasbaoui, B., Fayssal, B. M. (2016). Novel Four Wheel Drive Propulsion System Control Using Backstepping Strategy. *Procedia Technology*, *22*, 509–517.

[17]. Yang, W., Zhou, X., Ju, B., Xu, P. (2012). Robust control of electric vehicle's driving system. *IEEE 2nd International Conference on Cloud Computing and Intelligence Systems.*

[18]. Boukhnifer, M., Chaibet, A., Ouddah, N., Monmasson, E. (2017). Speed robust design of switched reluctance motor for electric vehicle system. *Advances in Mechanical Engineering*, *9*(11).

[19]. Ali, S. M. N., Hossain, J., Wang, D., Lu, K., Rasmussen, P. O., Sharma, V., & Kashif, M. (2020). Robust Sensorless Control Against Thermally Degraded Speed Performance in an IM Drive Based Electric Vehicle. IEEE Transactions on Energy Conversion, 1–1.

[20]. Boukhnifer, M., Chaibet, A., Ouddah, N., Monmasson, E. (2017). Speed robust design of switched reluctance motor for electric vehicle system. *Advances in Mechanical Engineering*, *9*(11).

[21]. J. Bürger, J. Anderson, (2019). Robust control for electric vehicle powertrains. *Computer Science Control Theory and Technology.*

[22]. Saadi, R., Hammoudi, M. Y., Kraa, O., Ayad, M. Y., & Bahri, M. (2019). A robust control of a 4- leg floating interleaved boost converter for fuel cell electric vehicle application. Mathematics and Computers in Simulation.

[23]. Zhao, W., & Zhang, H. (2018). Coupling Control Strategy of Force and Displacement for Electric Differential Power Steering System of Electric Vehicle With Motorized Wheels. *IEEE Transactions on Vehicular Technology, 67*(9), 8118–8128.

[24]. van der Schaft, A. J. (1992). L2 -gain analysis of nonlinear systems and nonlinear systems and nonlinear state feedback H1 control. *IEEE Transactions on Automatic Control*, vol. *37*, pp. 770 784.

[25]. van der Schaft, A.J.(1996). L2-gain and Passivity Techniques in Nonlinear Control. *Springer, London*.

[26]. Zhou, K., Doyle, J. C., Glover, K.(1996). Robust and optimal control. *Upper Saddle River, NJ: Prentice-Hall.*

[27]. Doyle, J.C., Glover, K., Khargonekar, P.P., Francis, B.A.(1989). State-space solutions to Standard H 2 and H∞ Control Problems.*IEEE Transactions on Automatic Control*, *34*(8), 831–847.

[28]. Skogesta, S., Postlethwaite, I. (2005). Multivariable Feedback Control Analysis and design, 2nd Edition.

[29].Cheng, T., & Lewis, F.L. (2007). Neural network solution for finite-horizon H-infinity constrained optimal control of nonlinear systems. *Journal of Control Theory and Applications*, *5*(1), 1–11.

[30]. Soares Longhi, L.G., Resende Secchi, A., Otávio Trierweiler, J., & Luis Lima, E. (2000). A Possible Approach to Solve Nonlinear H-Infinity Control Problem. *IFAC Proceedings* Volumes, *33*(10), 887–892.

[31]. Luo, B., Wu, H.-N., & Huang, T. (2015). Off-Policy Reinforcement Learning for H∞ Control Design. *IEEE Transactions on Cybernetics*, *45*(1), 65–76.

[32]. Bachir Bouiadjra, R., Khelfi, M.F., Salem, M., & Sedraoui, M. (2016). Nonlinear H ∞ control via measurement feedback using neural network. *Journal of the Brazilian Society of Mechanical Sciences and Engineering*, *39*(4), 1109–1118.

[33]. Meng, F., Wang, D., Yang, P., & Xie, G. (2019). Application of Sum of Squares Method in Nonlinear H∞ Control for Satellite Attitude Maneuvers. Complexity, 2019, 1–10.

[34]. Ferreira, H. C., Rocha, P. H., & Sales, R. M. (2008). Nonlinear H∞ control and the Hamilton-Jacobi-Isaacs equation. *IFAC Proceedings* Volumes, *41*(2), 188–193.

[35]. Beard, R., G. Saridis, Wen J. (1998). Approximate Solutions to the Time-Invariant Hamilton-Jacobi-Bellman Equation. *Journal of Optimization Theory and Application*, *96*(3): 589-626.

[36]. Beard, R., Saridis G., Wen J. (1997). Galerkin Approximations of the Generalized Hamilton-Jacobi-Bellman Equation. *Automatica, 33*: 12, pp. 2159-2177.

[37]. Beard, R., McLain, T. (1998). Successive Galerkin approximation algorithms for nonlinear optimal and robust control. *International Journal of Control*, *71(*5), 717-743.

[38]. Qu, Z.Y., Ye, Z.M. (2011). Simulation Studies on Model Reference Adaptive Controller for Permanent Magnet Synchronous Motor Drive. *Advanced Materials Research*, 268-270, 509–512.

[39]. Sharma, R. K., Sanadhya, V., Behera, L., and Bhattacharya, S. (2008). Vector control of a permanent magnet synchronous motor. *Annual IEEE India Conference*.

[40]. Li, S., Haskew, T.A., Hong, Y. (2012). Characteristic study of vector-controlled permanent magnet synchronous motor in electric drive vehicles. *IEEE PES Transmission and Distribution Conference and Exposition(T&D 2012), Orlando, Florida, USA.*

[41]. Do, T.D., Choi, H.H., & Jung, J.W. (2012). SDRE-Based Near Optimal Control System Design for PM Synchronous Motor. *IEEE Transactions on Industrial Electronics*, 59(11), 4063–4074.

[42]. Do, T.D., Choi, H.H., & Jung, J.W. (2015). θ-D Approximation Technique for Nonlinear Optimal Speed Control Design of Surface-Mounted PMSM Drives. *IEEE/ASME Transactions on Mechatronics*, *20*(4), 1822–1831.